# Optimization in Liquid-Vapor Region for Cryogenic based Separation Simulation of Natural Gas Components

Open Access

Ali Qasim[1], Bhajan Lal[1,*], Muhammad Babar[1], Abulhassan Ali[1], Mohamad Azmi Bustam[1], Azmi Mohd Shariff[1]

[1] Chemical Engineering Department, Universiti Teknologi PETRONAS, Tronoh, Perak, 31750, Malaysia

| ARTICLE INFO | ABSTRACT |
|---|---|
| | The liquid-vapor (L-V) and solid-vapor (S-V) domains of the natural gas mixture with high CO2 content and heavier hydrocarbons up to pentane for cryogenic separation have been obtained through simulation. The simulations are performed using Aspen HYSYS. The pressure-temperature phase diagram is generated for selected gaseous mixtures and the phase boundaries of both liquid-vapor region and solid-vapor region are identified. Optimized pressure and temperature conditions in liquid-vapor region have been found using response surface methodology through Design-Expert software. For gas mixture 1, the first set of condition from two set of optimized conditions for pressure and temperature is 38.04 bar and 0 °C while the second set of condition constitutes of 9.92 bar and -30 °C. The optimum pressure and temperature conditions for gas mixture 2 are 38.67 bar, 0 °C and 6.95 bar, -30 °C. |
| | |

## 1. Introduction

The interest for oil, petroleum gas, and other sources is developing significantly as it is assessed that overall energy utilization will increment to over 40% by 2035 [1-2]. The developing interest is additionally filled by a regularly expanding populace [3-4]. Petroleum gas is the biggest single contributor of the world's aggregate energy requirements as it is utilized as a part of residential warming purposes and furthermore for power generation and is considered to be a clean fuel [5]. It is determined that 33% of all the petroleum gas holds are acrid and Malaysia alone have some flammable gas reserves wherein the $CO_2$ content is more than 70 % [5]. The high amount of $CO_2$ in natural gas increases the formation of carbonic acid and dry ice thus causing erosion and disrupting delivery pipelines. Consequently, the expulsion of $CO_2$ from the natural gas is critical to improve the calorific value of the gas [6-7].

With the ever-increasing population and energy consumption, it is important to develop advanced and economical technologies to build up an efficient procedure for carbon dioxide removal

---

* Corresponding author.
E-mail address: bhajan.lal@utp.edu.my (Bhajan Lal)

from gas streams with high $CO_2$ content natural gas reserves [8-10]. The cryogenic technique is a developing innovative method for carbon dioxide capture and natural gas cleaning, so it requires an adequate research for future applications [11]. Cryogenics separation study involves the separation of natural gas mixture constituents at lower temperatures. Cryogenics technology is advantageous over other existing amine absorption or adsorption based processes as no solvents are required in the process, makeup water supply for the process is not needed, equipment for solvent regeneration is also not needed and $CO_2$ is available at higher pressure. The $CO_2$ obtained can be used for Enhanced Oil Recovery or sequestration purposes. In addition, Natural Gas Liquids (NGL) are obtained as a by-product which have good market potential. In hybrid cryogenic separation process, conventional flash separators are used in conjunction with de-sublimation based packed bed separators. It has an added advantage of reduced energy requirement along with the reduced equipment size. The identification of temperature and pressure ranges in hybrid application can prove to be beneficial for further design and optimization of the process [12-13].

In this work, liquid-vapor (L-V) and solid-vapor (S-V) domains for hybrid cryogenic separation process have been identified through simulation. The phase behavior is determined using Peng-Robinson EoS and the bubble point, dew point and freeze out curves are obtained for multicomponent natural gas mixture. The optimized points in liquid-vapor domain for maximum $CO_2$ separation in vapor phase and $C_5H_{12}$ in liquid phase have also been determined. In liquid-vapor domain, $CO_2$ is maximally separated in vapor form while the maximum content of heavier hydrocarbons as pentane is separated in liquid product. The $CO_2$ separated in vapor phase can be desublimated in solid-vapor region while pentane separated as liquid in liquid-vapor region is obtained as a valuable product to be put into commercial use. The investigation of phase behavior with the identification of optimized pressure and temperature conditions in liquid-vapor and solid-vapor regions can be used to develop an economically efficient process in cryogenic application for the separation of natural gas components using hybrid cryogenic technique.

## 2. Methodology
### 2.1 VLE Behavior Estimation

In order to identify the phase regions, feed gas includes natural gas with high $CO_2$ content comprising of methane to pentane as shown in Table 1. The composition is based on the maximum possible amount of heavier hydrocarbons that exists in Malaysia natural gas mixture containing high carbon dioxide content [14].

**Table 1**
Natural gas feed streams composition [14]

| Component | Composition (Mol %) | |
|---|---|---|
| | Gas Mixture 1 | Gas mixture 2 |
| $CH_4$ | 30 | 20 |
| $CO_2$ | 60 | 70 |
| $C_2H_6$ | 5 | 5 |
| $C_3H_8$ | 2.8 | 2.8 |
| $C_4H_{10}$ | 1.2 | 1.1 |
| $C_5H_{12}$ | 1 | 1 |

The pressure temperature phase diagram is generated in Aspen HYSYS 8.0. The phase behavior is investigated through the generation of bubble point and dew point curves along with the $CO_2$ freeze out. The validation of Peng-Robinson equation state has been used to generate phase diagram for the selected feed streams as in the case of hydrocarbon gaseous mixture, the VLE behavior prediction is the most accurate [14]. The validation for the use of software has been performed by comparing the experimental solid-liquid-vapor (SLV) locus for $CO_2$/$CH_4$ binary gas mixture with the values predicted by HYSYS for SLV locus. The total inlet molar flow rate for both the gas mixtures is kept at 100 kmol/h. The molar flow rate for gas mixture 1, when converted to mass flow rate is equivalent to 3537.6 kg/h. For gas mixture 2, the total mass flow rate is 3817.26 kg/h.

## 2.2 Optimized Experimental Conditions for L-V Domain

For optimization, the objective is to maximize the amount of $CO_2$ in vapor and minimize the amount of $C_5H_{12}$ in vapor at the top product with minimum energy consumption. The pentane content in vapor is minimized at the top for efficient separation purposes so that the maximum content of it should be available in liquid at the bottom. The $CO_2$ in vapor at the top can further be desublimated onto the surface of the packed bed while pentane obtained as liquid in bottom product for hybrid cryogenic separation technique. The parameters to be optimized have been calculated in terms of cost. For optimization, the mass flow rates and required duty are converted in terms of money throughput. It is done by taking the product of mass flow rate (kg/h) with the price per kg of the gases and the product of energy consumption (KJ/h) with the consumed energy price which is price per kilojoule, respectively. The price is considered in Malaysian national currency, Ringgit, abbreviated as RM. Optimization has been performed using Design-Expert software to find the most feasible points for future experimentation and to find the appropriate temperature and pressure conditions inside the liquid vapor domain. The software employs response surface methodology as optimization technique to find out the optimized set of points that are confined within the range of liquid-vapor domain. Furthermore, the separation of natural gas components can be done at the pressure and temperature conditions at these particular conditions obtained through optimization. The optimization is performed in Design-Expert software using response surface methodology. Response surface methodology (RSM) is a statistical technique used for the optimization of complicated processes due to its efficient arrangements of experiments [12-13]. Central Composite Design (CCD) is the widely used approach in response surface methodology. CCD is based on quadratic model for response variable. RSM has been used in recent studies involving $CO_2$ capture. Guerrero *et al.,* investigated the effect of temperature, pressure and feed flow rate on $CO_2$ desorption for adsorbent regeneration purposes involving amine based adsorption process. The effect of these variables on the desorption rate and regeneration performance was approached and studied using RSM [14]. Based on ANOVA results, Central Composite Face-centered (CCF) design is used because of higher value of coefficient of determination.

## 3. Results and Discussion
### 3.1 Validation of the SLV Phase Behavior for $CO_2$/$CH_4$ Gas Mixture

The Solid-Liquid-Vapor (SLV) locus has been validated using Aspen HYSYS simulator with the data available in literature where the three phase data has been determined experimentally for $CO_2$-$CH_4$ gas system. The three phase locus is measured over the temperature range of -78.6 °C to -57.8 °C. The simulated data match well with the experimental data produced by Donnelly and others [15]. It

can be noticed from the Table 2 that at lower temperatures the phase starts shifting from liquid-vapor domain to solid-vapor domain with the increase in pressure.

### 3.1.1 Phase behavior of natural gas mixtures

Figure 1 shows the pressure-temperature phase diagram for natural gas mixture for the selected feed stream compositions mentioned in Table 1 which identify the solid, liquid and vapor regions for the study. The regions in which separation can be performed are mentioned in Figure 1. It can be seen that the L-V region starts from about 0 °C to -60 °C and S-V domain lies in the temperature range of -60 °C to -120°C. Bubble point and dew point curves have been obtained for the natural gas feed containing 60% and 70% $CO_2$ in feed along with higher hydrocarbons ranging from methane to pentane. The $CO_2$ freeze out curve has also been determined.

**Table 2**
AAE of experimental and predicted temperature values for SLV locus [15]

| P (bar) | Experimental T ( °C) | Predicted T( °C) | AAE (%) |
|---------|---------|---------|---------|
| 9.04 | -57.7 | -60.0 | 3.84 |
| 10.74 | -58.3 | -57.8 | 0.91 |
| 12.85 | -57.5 | -58.2 | 1.21 |
| 18.02 | -59.1 | -59.3 | 0.22 |
| 24.35 | -59.7 | -60.6 | 1.47 |
| 29.72 | -60.5 | -61.7 | 1.89 |
| 31.29 | -61.1 | -62.1 | 1.61 |
| 32.04 | -61.3 | -62.3 | 1.48 |
| 38.09 | -61.3 | -62.7 | 2.13 |
| 39.59 | -61.6 | -63.0 | 2.16 |
| 40.20 | -62.2 | -63.2 | 1.57 |
| 41.83 | -63.0 | -64.6 | 2.44 |
| 44.28 | -62.7 | -64.0 | 1.94 |
| 44.62 | -63.0 | -64.3 | 1.97 |
| 44.96 | -64.1 | -65.6 | 2.23 |
| 46.93 | -64.7 | -65.3 | 0.89 |
| 47.89 | -66.9 | -66.7 | 0.36 |
| 46.46 | -69.7 | -68.8 | 1.24 |
| 44.76 | -71.1 | -70.7 | 0.50 |
| 43.06 | -72.7 | -71.6 | 1.50 |
| 37.55 | -78.6 | -78.1 | 0.57 |

It can be seen from Figure 1 that at higher temperatures as 40 °C to 0 °C, the gas mixture is in vapor state. It can also be noticed that the vapor-liquid region lies in the temperature range of 0 to -60 °C and beyond -60 °C to about -120 °C, the phase enters into solid-vapor region. At high pressures above 40 bar and above the $CO_2$ freeze out temperature, the phase lies in liquid region. At very low temperatures as -120 °C and lower than this and at moderate pressures, it enters into solid-liquid region. It is feasible to do separation in liquid-vapor and solid-vapor domains as energy requirements to lower the temperatures to solid-liquid region become high. After identification of the domains, the separation of components can be done by using hybrid cryogenic technique.
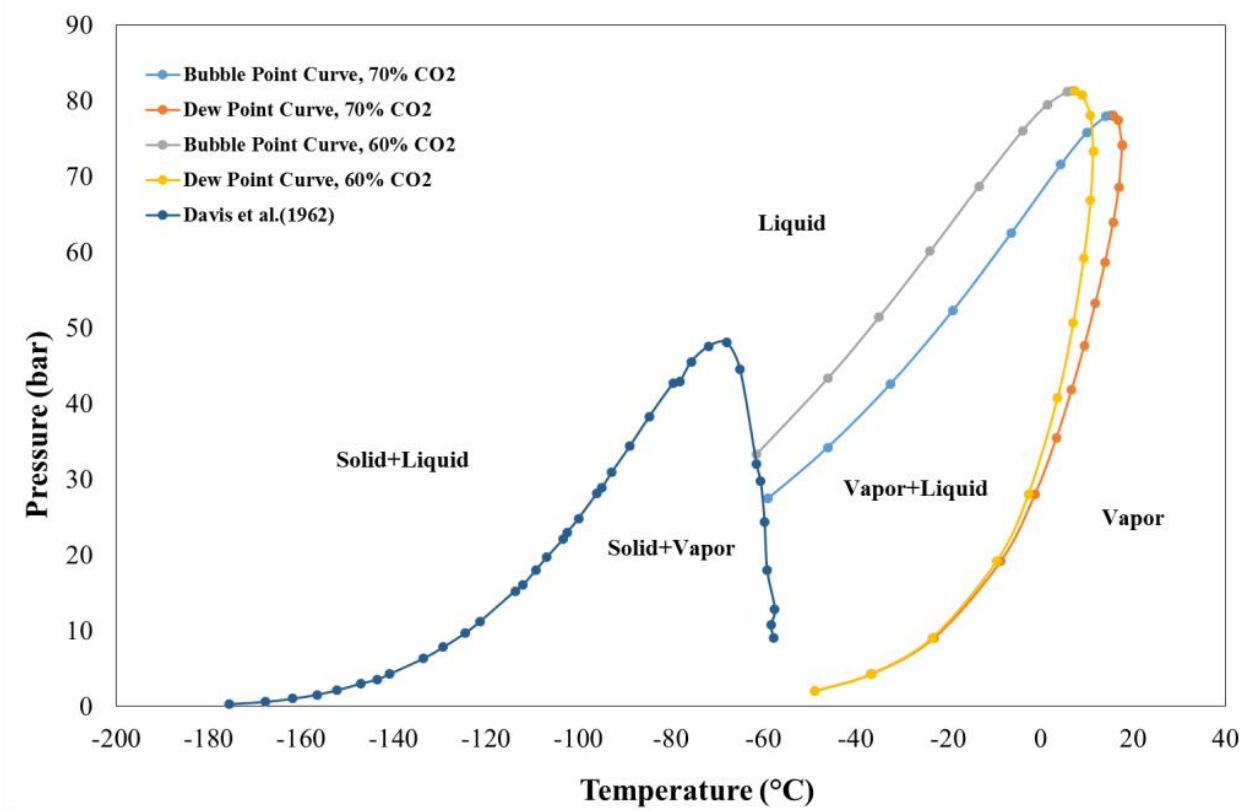
**Fig. 1.** Pressure-Temperature phase diagram for Natural Gas Mixture

## 3.2 Results of Analysis for Gas Mixture 1

The optimized conditions for gas mixture 1 having $CO_2$ MFR in feed was about 2640.58 kg/h within the liquid-vapor domain as predicted through RSM are presented in Table 3.The mass flow rate of $CO_2$ in feed is 2640.58 kg/h and $C_5H_{12}$ is 72.151 kg/h . For gas mixture 1, a total of 13 set of conditions of pressure and temperature are obtained using RSM technique through central composite design (CCD). The conditions according to factorial design are shown in Table 4. The pressure and temperature conditions are mentioned in terms of coded and actual values obtained in Design-Expert software. The actual values are abound in between liquid-vapor range of the phase and coded values represent the minimum, maximum and average values in between the L-V range.

**Table 3**
Optimized values obtained through RSM for gas mixture 1

| P (bar) | T (°C) | $CO_2$ vapor MFR(kg/h) | $CO_2$ recovery rate (RM/h) | $C_5H_{12}$ vapor MFR (kg/h) | $C_5H_{12}$ recovery rate (RM/h) | Energy Cost (RM/h) |
|---------|--------|------------------------|------------------------------|-------------------------------|----------------------------------|--------------------|
| 38.04 | 0 | 2560.6 | 5505.42 | 31.27 | 134.46 | 29.71 |
| 9.92 | -30 | 2524.5 | 5427.62 | 32.81 | 141.11 | 30.88 |

**Table 4**
Coded and actual values for gas mixture 1

| Coded value | | Actual value | |
|---|---|---|---|
| T | P | T (°C) | P (bar) |
| -1 | 0 | -30 | 22.5 |
| -1 | -1 | -30 | 5 |
| 0 | 0 | -15 | 22.5 |
| 0 | 0 | -15 | 22.5 |
| +1 | 0 | 0 | 22.5 |
| 0 | 0 | -15 | 22.5 |
| -1 | +1 | -30 | 40 |
| 0 | 0 | -15 | 22.5 |
| 0 | 0 | -15 | 22.5 |
| 0 | -1 | -15 | 5 |
| +1 | -1 | 0 | 5 |
| 0 | +1 | -15 | 40 |
| +1 | +1 | 0 | 40 |

### 3.2.1 Optimization of $CO_2$ recovery rate

Table 5 shows the ANOVA results for $CO_2$ recovery rate for gas mixture 1. The coefficient of determination, R-squared, values show the goodness of the model used to predict the optimized values. The measures of R-squared and adjusted R-squared are close to 1 which indicates a suitable model. Probability or p-value is the measure of how much the particular event can occur as chance. A small p-value typically ≤ 0.05 indicates strong evidence against the null hypothesis, so null hypothesis can be rejected and the model is significant. A large p-value of > 0.05 indicates weak evidence against the null hypothesis and renders model insignificant.

**Table 5**
ANOVA for CO2 recovery rate for gas mixture 1

| Source | Sum of Squares | df | Mean Square | F Value | p-value | Significance |
|---|---|---|---|---|---|---|
| Model | $2.07*10^7$ | 5 | $4.14E*10^6$ | 72.24 | < 0.0001 | Significant |
| A-P | $7.68*10^6$ | 1 | $7.68E*10^6$ | 133.9 | < 0.0001 | |
| B-T | $5.48*10^6$ | 1 | $5.48*10^6$ | 95.51 | < 0.0001 | |
| AB | $4.79*10^6$ | 1 | $4.79*10^6$ | 83.42 | < 0.0001 | |
| A^2 | $1.49*10^6$ | 1 | $1.49*10^6$ | 26.02 | $1.40*10^{-3}$ | |
| B^2 | $3.38*10^5$ | 1 | $3.38*10^5$ | 5.89 | $4.56*10^{-2}$ | |
| Residual | $4.02*10^5$ | 7 | $57370.0^8$ | | | |
| Lack of Fit | $4.02*10^5$ | 3 | $1.34*10^5$ | | | |
| Pure Error | 0 | 4 | 0 | | | |
| Cor Total | $2.11*10^7$ | 12 | | | | |
| R-Squared: | | | | 0.981 | | |
| Adj R-Squared: | | | | 0.970 | | |

The 3-D surface plots for optimzed conditions of $CO_2$ recovery parametric conditions from Table 3 are depicted in the following section in Figure 2. Surface plots help to visualize the relationship between the process parameters and accordingly responses in order to examine the optimum conditions.

The surface plots of $CO_2$ recovery rate for gas mixture 1 are shown in Figure 2. The determination coefficient, $R^2$, shows the goodness of fit of the polynomial model, which in this case has a satisfactory

value of 0.981. As the flowrate is kept constant, it is the effect of pressure and temperature which affects the recovery of $CO_2$. At a pressure of 38.04 bar and temperature 0 °C, in terms of mass flowrate, the amount of $CO_2$ being removed in vapor is 2560.6 kg/h from a total amount of 2640.6 kg/h in feed. It shows that the 97% of the $CO_2$ from the total amount is available in the required vapor phase. At pressure equals to 9.92 bar and temperature of -30 °C, the amount of $CO_2$ in vapor state in top product is about 96% of the total feed of $CO_2$ which indicates an efficient process at these conditions for $CO_2$ separation.
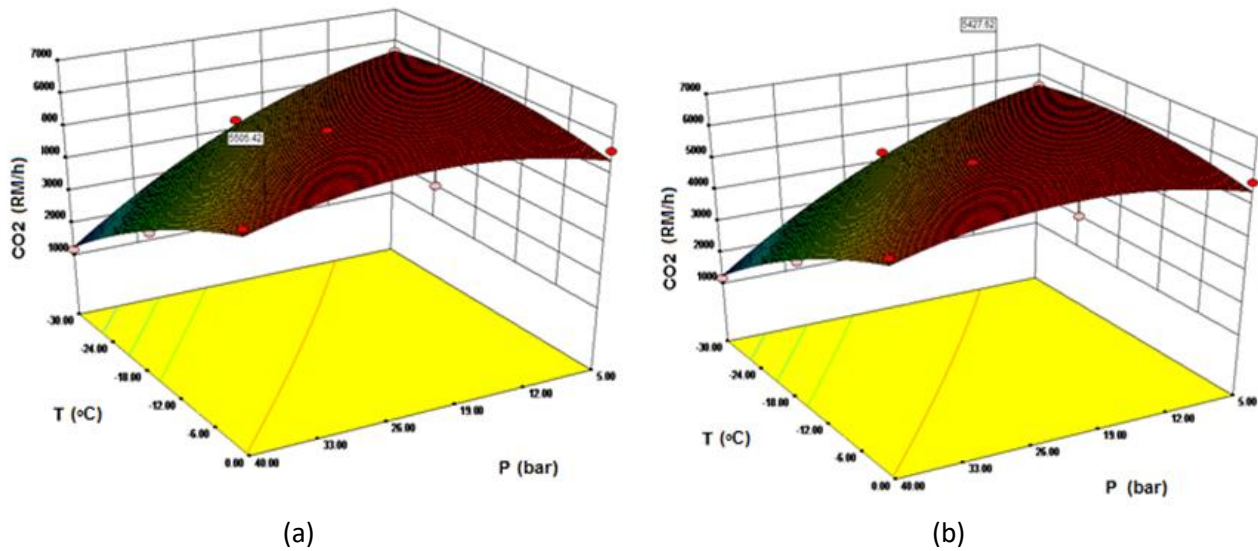


Fig. 2. 3-D Surface plots for $CO_2$ rate at (a) *P*=38.04 bar, *T*=0 °C, (b) *P*=9.92 bar, *T*=-30 °C

The predicted model of $CO_2$ recovery for feed composition of gas mixture 1 is obtained by the following second-order polynomial function. The final equation in terms of actual factors for $CO_2$ recovery is stated as follows. The recovery is in terms of cost.

$$CO_2 \text{ recovery rate (RM/h)} = 4952 + (105.8P) - (76.7T) + (4.16PT) - (2.4P^2) - (1.55T^2) \qquad (1)$$

Figure 3 shows the $C_5H_{12}$ recovery rate for gas mixture 1 at the specified conditions of presure and temperature. At a first set of conditions of 0 °C and 38.04 bar, the amount of $C_5H_{12}$ being removed in liquid is about 57% of the total amount of feed while the rest of $C_5H_{12}$ is in vapor phase. It is the maximum amount of separation for $C_5H_{12}$ that can be achieved at the mentioned coditions of pressure and temperature. While at the pressure of 9.92 bar at -30 °C, the amount of $C_5H_{12}$ in the required liquid phase is 54.53% of the overall amount in feed.
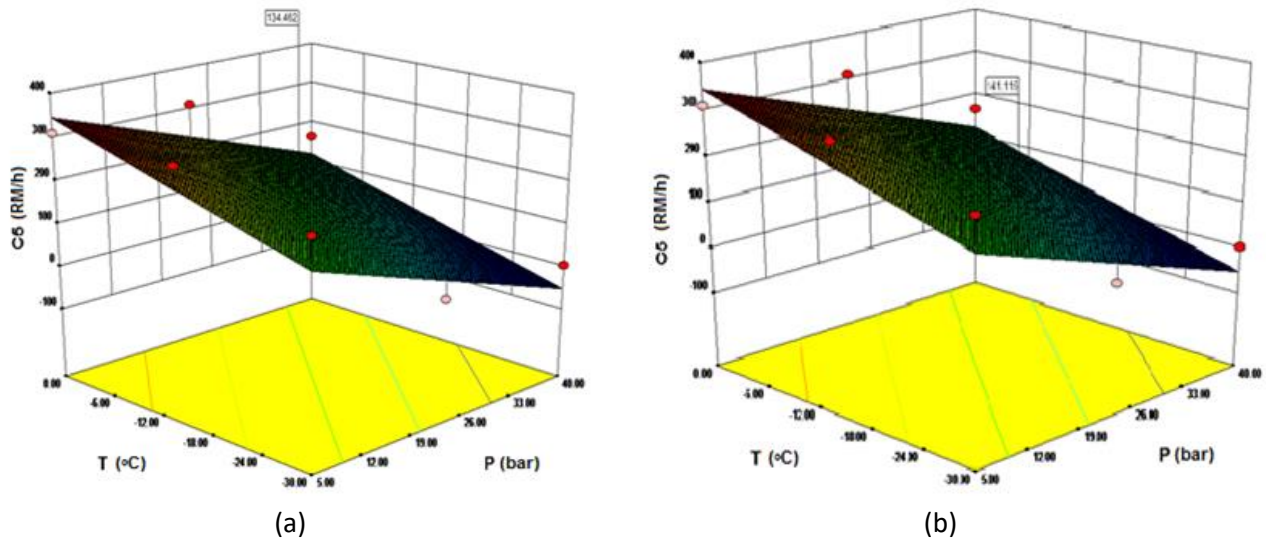
**Fig. 3.** 3-D Surface plots for $C_5H_{12}$ rate at (a) *P*=38.04 bar, *T*=0 °C, (b) *P*=9.92 bar, *T*=-30 °C

### 3.2.2 Optimization of $C_5H_{12}$ recovery rate

For $C_5H_{12}$ recovery rate, the ANOVA results are given in Table 6. The model is significant with the R-squared value of 0.8. In case of separation of $C_5H_{12}$, the value of R-squared is 0.8 which although is less than that of in the case of $CO_2$ but lies in acceptable bounds. $C_5H_{12}$ in required phase is slightly better at first set of conditions from Table 3 as compared to that of second set of conditions.

The equation predicted for pentane recovery rate for gas mixture 1 can be given as follows.

$$C_5H_{12} \text{ recovery rate (RM/h)} = 377.5 - (6.38P) + (5.76T)$$

(2)

**Table 6**
ANOVA for C5H12 recovery rate for gas mixture 1

| Source | Sum of Squares | df | Mean Square | F Value | p-value | Significance |
|---|---|---|---|---|---|---|
| Model | 119903.8 | 2 | 59951.9 | 19.60029 | 0.0003 | significant |
| A-P | 74992.06 | 1 | 74992.06 | 24.51742 | 0.0006 | |
| B-T | 44911.73 | 1 | 44911.73 | 14.68315 | 0.0033 | |
| Residual | 30587.25 | 10 | 3058.725 | | | |
| Lack of Fit | 30587.25 | 6 | 5097.875 | | | |
| Pure Error | 0 | 4 | 0 | | | |
| Cor Total | 150491 | 12 | | | | |
| R-Squared: | | | 0.800 | | | |
| Adj R-Squared: | | | 0.760 | | | |

### 3.2.3 Optimization of energy cost

The R-squared value for energy cost in case of gas mixture 2 is 0.995 and the model is significant. The ANOVA results are shown in Table 7.

The 3-D surface plots of optimized conditions of energy cost or required duty cost for the both set of conditions given in Table 7 are shown in Figure 4.

**Table 7**
ANOVA for energy cost for gas mixture 1

| Source | Sum of Squares | df | Mean Square | F Value | p-value | Significance |
|---|---|---|---|---|---|---|
| Model | 7004.97 | 5 | 1400.99 | 290.75 | < 0.0001 | significant |
| A-P | 3459.64 | 1 | 3459.64 | 717.99 | < 0.0001 | |
| B-T | 2335.55 | 1 | 2335.55 | 484.71 | < 0.0001 | |
| AB | 842.55 | 1 | 842.55 | 174.86 | < 0.0001 | |
| A^2 | 171.07 | 1 | 171.07 | 35.5 | 0.0006 | |
| B^2 | 63.47 | 1 | 63.47 | 13.17 | 0.0084 | |
| Residual | 33.73 | 7 | 4.82 | | | |
| Lack of Fit | 33.73 | 3 | 11.24 | | | |
| Pure Error | 0 | 4 | 0 | | | |
| Cor Total | 7038.7 | 12 | | | | |
| R-Squared: | | | 0.995 | | | |
| Adj R-Squared: | | | 0.992 | | | |

The equation for required duty is also a second degree polynomial equation which is described below.

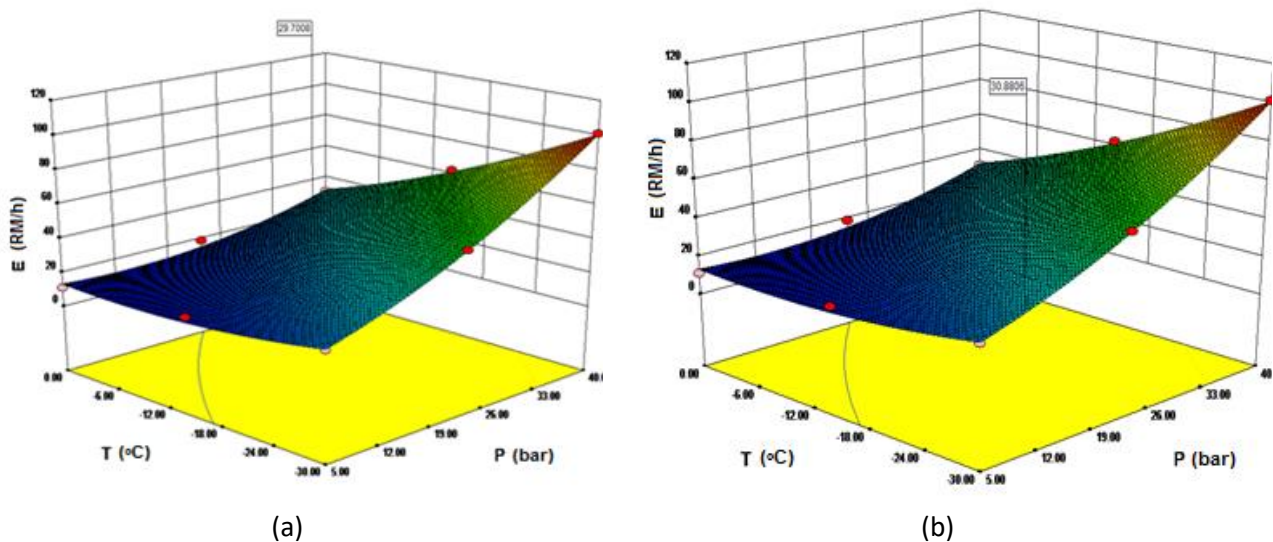$$\text{Duty required, E (RM/h)} = 15.85 - (0.61P) + (0.567T) - (0.055T) + (0.257P^2) - (0.02T^2)$$

(3)



(a)                                                                 (b)

**Fig. 4.** 3-D Surface plots for Energy cost at (a) *P*=38.04 bar, *T*=0 °C, (b) *P*=9.92 bar, *T*=-30 °C

### 3.3 Results of Analysis for Gas Mixture 2

The optimized conditions for the gas feed mixture, gas mixture 2, containing 70% $CO_2$ and remaining hydrocarbons is found similarly and is summarized in Table 8. The $CO_2$ feed mass flow rate is 3080.68 kg/h and $C_5H_{12}$ mass flow rate is 72.15 kg/h. A total of 13 set of conditions of pressure and temperature are recommended in central composite design (CCD) to probe the values of response variables. According to the factorial design, the conditions are shown in Table 9. The parametric conditions are given in terms of coded and actual values obtained in the software. The actual values are in between liquid-vapor range of the phase and coded values represent the minimum, maximum and average values in between the L-V domain.

**Table 8**
Optimized values obtained through RSM for gas mixture 2

| P (bar) | T (°C) | $CO_2$ vapor MFR(kg/h) | $CO_2$ recovery rate (RM/h) | $C_5H_{12}$ vapor MFR (kg/h) | $C_5H_{12}$ recovery rate (RM/h) | Energy Cost (RM/h) |
|---|---|---|---|---|---|---|
| 38.67 | 0 | 2913.5 | 5860.55 | 30.35 | 100.38 | 29.95 |
| 6.95 | -30 | 3072.7 | 6158 | 35.85 | 164 | 25 |

**Table 9**
Coded and actual values for gas mixture 2

| Coded values | | Actual values | |
|---|---|---|---|
| T (°C) | P (bar) | T (°C ) | P (bar) |
| 0 | 0 | -15 | 22.5 |
| -1 | +1 | -30 | 40 |
| 0 | +1 | -15 | 40 |
| 0 | 0 | -15 | 22.5 |
| +1 | -1 | 0 | 5 |
| 0 | -1 | -15 | 5 |
| 0 | 0 | -15 | 22.5 |
| +1 | 0 | 0 | 22.5 |
| -1 | -1 | -30 | 5 |
| -1 | 0 | -30 | 22.5 |
| 0 | 0 | -15 | 22.5 |
| +1 | +1 | 0 | 40 |
| 0 | 0 | -15 | 22.5 |

### 3.3.1 Optimization of $CO_2$ recovery rate

The results of ANOVA for $CO_2$ recovery rate are shown in Table 10. The R-squared values given by the model involved in the optimization of process variable for gas mixture 2 is 0.926 which is closer to 1 so it shows the use of an adequate model.

**Table 10**
ANOVA for $CO_2$ recovery rate for gas mixture 2

| Factors | Sum of Squares | df | Mean Square | F Value | P-value | Significance |
|---|---|---|---|---|---|---|
| Model | $5.10*10^7$ | 5 | $1.02*10^7$ | 17.5 | 0.0008 | Significant |
| A-T | $1.49*10^7$ | 1 | $1.49*10^7$ | 25.65 | 0.0015 | |
| B-P | $2.16*10^7$ | 1 | $2.16*10^7$ | 37.09 | 0.0005 | |
| AB | $8.49*10^6$ | 1 | $8.49*10^6$ | 14.58 | 0.0066 | |
| A^2 | $8.71*10^5$ | 1 | $8.71*10^5$ | 1.5 | 0.261 | |
| B^2 | $2.97*10^6$ | 1 | $2.97*10^6$ | 5.1 | 0.0586 | |
| Residual | $4.08*10^6$ | 7 | $5.82*10^5$ | | | |
| Lack of Fit | $4.08*10^6$ | 3 | $1.36*10^6$ | | | |
| Pure Error | 0 | 4 | 0 | | | |
| Cor Total | $5.50*10^7$ | 12 | | | | |
| R-Squared: | | | 0.926 | | | |
| Adj R-Squared: | | | 0.873 | | | |

The 3-D surface plots for $CO_2$ recovery rate at both set of conditions of Pressure and Temperature mentioned in Table 8 are given in Figure 5. The plots represent the optimum values of $CO_2$ recovery rate at respective pressure and temperature values as given in Table 8.
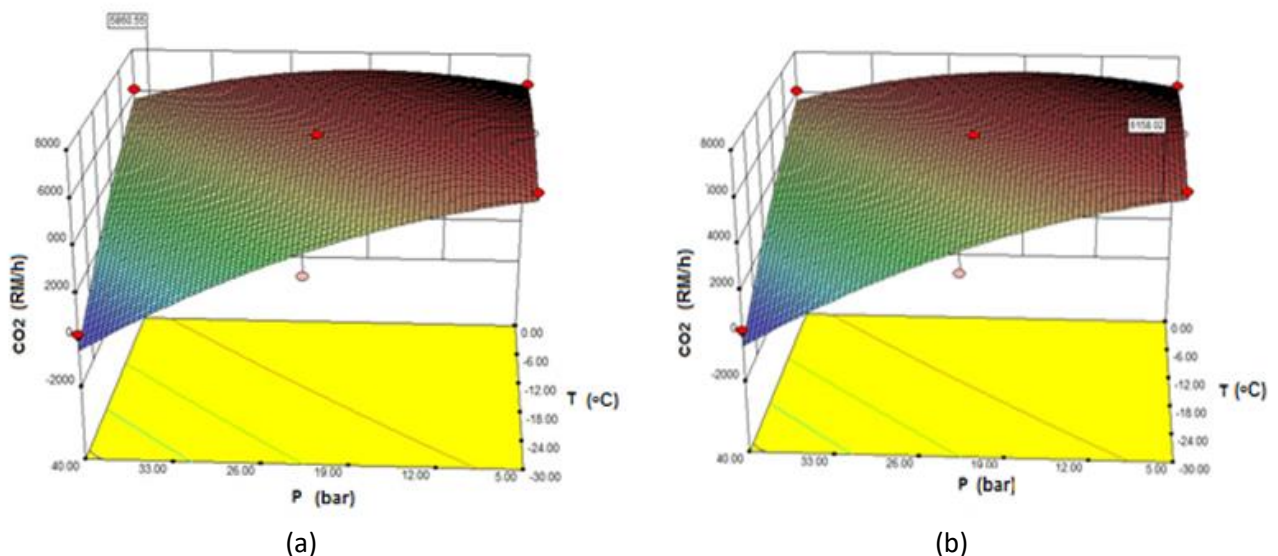


**Fig. 5.** 3-D Surface plots for $CO_2$ recovery rate at (a) *P*=38.67 bar, *T*=0 °C, (b) *P*=6.95 bar, *T*=-30 °C

For $CO_2$ recovery rate, the value for the determination coefficient, $R^2$, is 0.926 which shows a good. In case of gas mixture 2, the total $CO_2$ feed flow rate is 3080.68 kg/h. The amount of $CO_2$ that is obtained in vapor product is 95 % of the total amount of $CO_2$ in feed at pressure of 38.67 bar and 0 °C. The separation efficiency of $CO_2$ in required vapor phase at pressure of 6.95 bar at -30 °C is 99.7 % which is higher than the percentage of separation obtained through first set of conditions. In case of $CO_2$ recovery in vapor phase, it is evident that the separation at lower temperature is high even if the value of pressure is not high.

For gas mixture 2, the final equation in terms of actual factors for $CO_2$ is predicted as:

$$CO_2 \text{ recovery rate (RM/h)} = 6004 - (94.56T) + (127.14P) + (5.55P*T) - (2.49T^2) - (3.38P^2) \qquad (4)$$

### 3.3.2 Optimization of $C_5H_{12}$ recovery rate

The ANOVA results for $C_5H_{12}$ recovery rate are as follows in Table 11. Considering gas mixture 2, the total amount of mass flow rate of $C_5H_{12}$ in feed is 72.15 kg/h and the mass flow rate in vapor phase at the pressure of 38.67 bar and temperature equals to 0 °C, is 30.35 kg/h. It shows that rest of $C_5H_{12}$ is available in desired liquid phase which constitutes about 58 % of the inlet $C_5H_{12}$ feed flow rate. While at the pressure of 6.95 bar and -30 °C, the amount of $C_5H_{12}$ in vapor is 35.85 kg/h which is high as compared to the first set of conditions. The amount of $C_5H_{12}$ obtained in liquid is 50 % of the total feed flow rate (Figure 6). It can be noticed from the amount of $C_5H_{12}$ acquired in liquid stream that the more amount of it is obtained at the higher temperature of 0 °C and higher pressure of 38.67 bar as compared to the second set of pressure and temperature conditions reported in Table 8.

**Table 11**
ANOVA for $C_5H_{12}$ recovery rate for gas mixture 2

| Factors | Sum of Squares | df | Mean Square | F Value | P-value | Significance |
|---|---|---|---|---|---|---|
| Model | $5.10*10^7$ | 5 | $1.02*10^7$ | 17.5 | 0.0008 | Significant |
| A-T | $1.49*10^7$ | 1 | $1.49*10^7$ | 25.65 | 0.0015 | |
| B-P | $2.16*10^7$ | 1 | $2.16*10^7$ | 37.09 | 0.0005 | |
| AB | $8.49*10^6$ | 1 | $8.49*10^6$ | 14.58 | 0.0066 | |
| A^2 | $8.71*10^5$ | 1 | $8.71*10^5$ | 1.5 | 0.261 | |
| B^2 | $2.97*10^6$ | 1 | $2.97*10^6$ | 5.1 | 0.0586 | |
| Residual | $4.08*10^6$ | 7 | $5.82*10^5$ | | | |
| Lack of Fit | $4.08*10^6$ | 3 | $1.36*10^6$ | | | |
| Pure Error | 0 | 4 | 0 | | | |
| Cor Total | $5.50*10^7$ | 12 | | | | |
| R-Squared: | | | | 0.902 | | |
| Adj R-Squared: | | | | 0.870 | | |



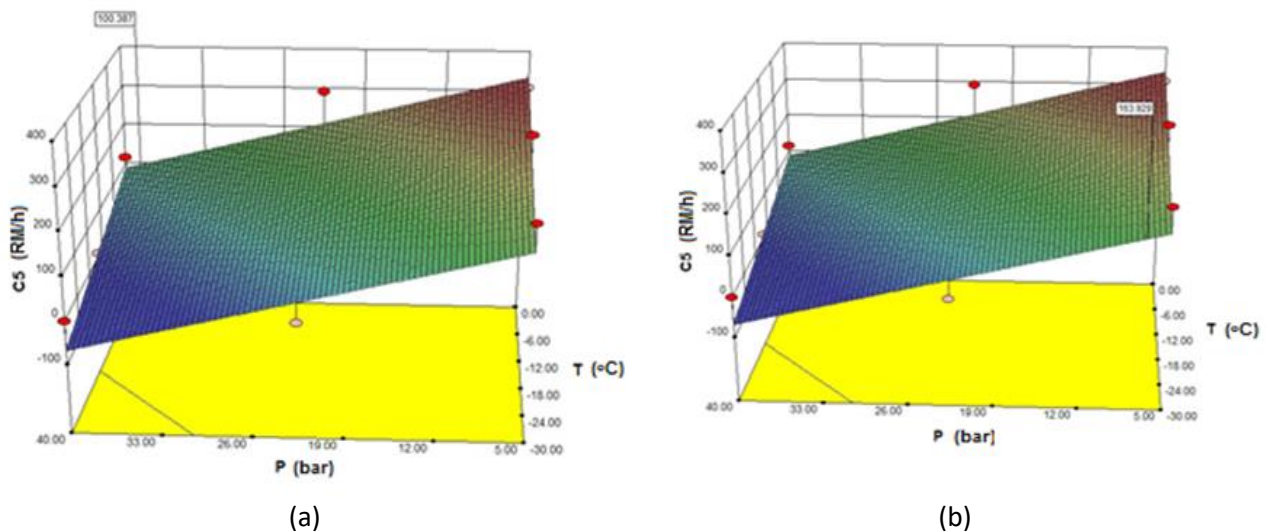(a)                                            (b)

**Fig. 6.** 3-D Surface plots for $C_5H_{12}$ recovery rate at (a) $P$=38.67 bar, $T$=0 °C, (b) $P$=6.95 bar, $T$=-30 °C

The surface plots for optimized conditions of energy cost for the set of conditions at P=38.67 bar, T= 0 °C and P=6.95 bar, T= -30 °C from Table 8 are given as in Figure 7.

It shows that the effect of pressure on $C_5H_{12}$ recovery is more compelling to that of temperature so high pressure favors the achievement of the desired condition. Figure 6 shows the surface plots of the optimized conditions at both sets of operational conditions from Table 8.

The predicted equation for $C_5H_{12}$ is described as

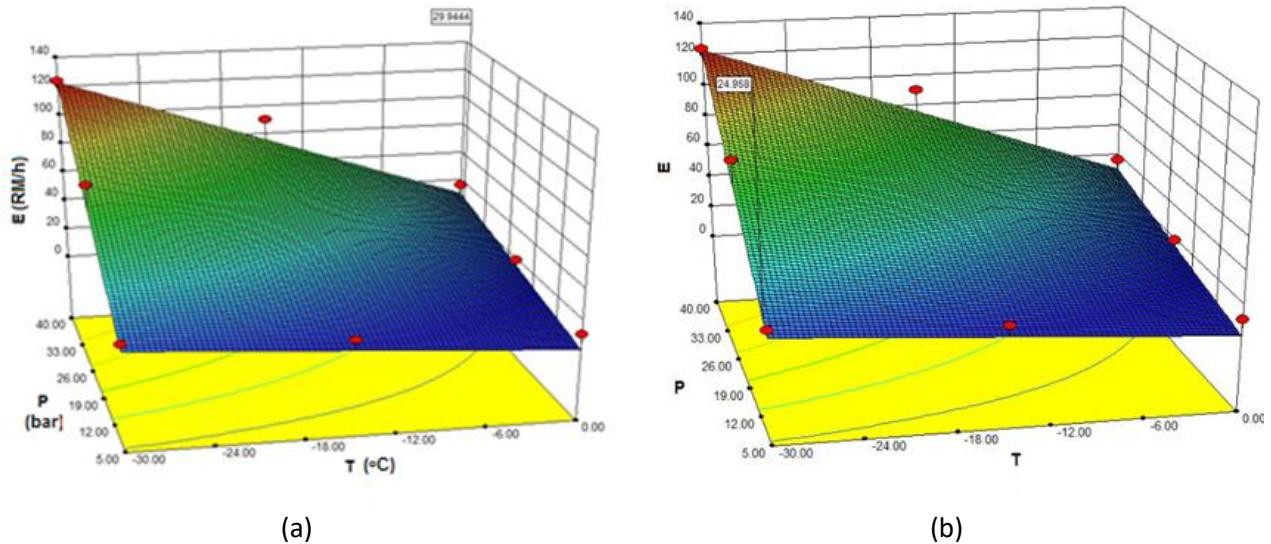$$C_5H_{12} \text{ recovery rate (RM/h)} = 370.27 + (5.26T) - (6.98P)$$

(5)

|           (a)           |           (b)           |

**Fig. 7.** 3-D Surface plots of Energy cost at (a) *P*=38.67 bar, *T*=0 °C, (b) *P*=6.95 bar, *T*= -30 °C

### 3.3.3 Optimization of energy cost

Table 12 presents the ANOVA results for the energy cost in case of gas mixture 2, while the surface plots are shown in Figure 7. The predicted equation for duty required is mentioned in Eq. (6).

$$\text{Duty required}, E\,(RM/h) = 2.94 - (0.24T) + (0.85P) - (0.071T*P) \tag{6}$$

**Table 12**
ANOVA for energy cost for gas mixture 2

| Source | Sum of Squares | df | Mean Square | F Value | p-value | Significance |
|--------|---------------|----|-------------|---------|---------|--------------|
| Model | 12645.73 | 3 | 4215.242 | 27.53008 | < 0.0001 | Significant |
| A-T | 4540.759 | 1 | 4540.759 | 29.65606 | 0.0004 | |
| B-P | 6722.717 | 1 | 6722.717 | 43.9066 | < 0.0001 | |
| AB | 1382.252 | 1 | 1382.252 | 9.027595 | 0.0148 | |
| Residual | 1378.026 | 9 | 153.114 | | | |
| Lack of Fit | 1378.026 | 5 | 275.6053 | | | |
| Pure Error | 0 | 4 | 0 | | | |
| Cor Total | 14023.75 | 12 | | | | |
| R-Squared: | | | | 0.803 | | |
| Adj R-Squared: | | | | 0.763 | | |

## 4. Conclusions

Liquid-vapor (L-V) and solid-vapor (S-V) regions for high $CO_2$ content natural gas have been identified through simulation. These regions are identified at cryogenic temperatures and high pressure conditions for two natural gas feed streams containing 60% and 70% $CO_2$ content respectively along with heavier hydrocarbons. The feed streams constituted hydrocarbon content ranging from methane to pentane. The temperature range for liquid-vapor domain extends from 0 °C to -60 °C with the pressure varying from 1 to 40 bar. At temperature of below -60 °C to -120 °C, the region is identified as solid-vapor region. In order to separate $CO_2$ in vapor form and pentane as liquid in L-V domain efficiently, optimization has been performed by using response surface methodology to identify the pressure and temperature conditions for maximum separation of carbon

dioxide in vapor phase while pentane in liquid phase with the minimization of energy. For both gas mixtures, two sets of optimum conditions of pressure and temperature have been proposed. For gas mixture 1, optimum pressure and temperature conditions in liquid-vapor region are 38.04 bar, 0 °C and 9.92 bar, -30 °C. In case of gas mixture 2, the optimized set of conditions comprise of 38.67 bar, 0 °C and 6.95 bar, -30 °C.

## Acknowledgement

## References
[1]   Fantazzini, Dean, Mikael Höök, and André Angelantoni. "Global oil risks in the early 21st century." *Energy Policy* 39, no. 12 (2011): 7865-7873.
[2]   Chu, Steven, and Arun Majumdar. "Opportunities and challenges for a sustainable energy future." *nature 488*, no. 7411 (2012): 294.
[3]   Johansson, Thomas B., Anand Prabhakar Patwardhan, Nebojša Nakićenović, and Luis Gomez-Echeverri, eds. Global energy assessment: toward a sustainable future. *Cambridge University Press*, 2012.
[4]   Asif, Muhammad, and Tariq Muneer. "Energy supply, its demand and security issues for developed and emerging economies." *Renewable and Sustainable Energy Reviews* 11, no. 7 (2007): 1388-1413.
[5]   Maqsood, Khuram, Aditi Mullick, Abulhassan Ali, Kajari Kargupta, and Saibal Ganguly. "Cryogenic carbon dioxide separation from natural gas: a review based on conventional and novel emerging technologies." *Reviews in Chemical Engineering* 30, no. 5 (2014): 453-477.
[6]   Darman, N. H., and A. R. B. Harun. "Technical challenges and solutions on natural gas development in Malaysia." *In The petroleum policy and management project*, 4th Workshop of the China-Sichuan Basin Study, Beijing, China. 2006.
[7]   Qasim, Ali, M. Zamri Abdullah, K. K. Lau, and Nor Adilla. "Flow Dynamics Investigation of CO2/CH4 Gas Mixture through Porous Media Using Computational Approach." In Applied Mechanics and Materials, vol. 625, pp. 369-372. *Trans Tech Publications*, 2014.
[8]   Maqsood, Khuram, Jayita Pal, Dhanaraj Turunawarasu, Anindya Jyoti Pal, and Saibal Ganguly. "Performance enhancement and energy reduction using hybrid cryogenic distillation networks for purification of natural gas with high CO2 content." *Korean Journal of Chemical Engineering* 31, no. 7 (2014): 1120-1135.
[9]   Hansen, James, Pushker Kharecha, Makiko Sato, Valerie Masson-Delmotte, Frank Ackerman, David J. Beerling, Paul J. Hearty *et al.,* "Assessing "dangerous climate change": required reduction of carbon emissions to protect young people, future generations and nature." *PloS one* 8, no. 12 (2013): e81648.
[10]  Goeppert, Alain, Miklos Czaun, Robert B. May, GK Surya Prakash, George A. Olah, and S. R. Narayanan. "Carbon dioxide capture from the air using a polyamine based regenerable solid adsorbent." *Journal of the American Chemical Society* 133, no. 50 (2011): 20164-20167.
[11]  Serna-Guerrero, Rodrigo, Youssef Belmabkhout, and Abdelhamid Sayari. "Influence of regeneration conditions on the cyclic performance of amine-grafted mesoporous silica for CO2 capture: An experimental and statistical study." *Chemical Engineering Science* 65, no. 14 (2010): 4166-4172.
[12]  Wu, Jianzhong, and John M. Prausnitz. "Phase equilibria for systems containing hydrocarbons, water, and salt: An extended Peng– Robinson equation of state." *Industrial & Engineering Chemistry Research* 37, no. 5 (1998): 1634-1643.
[13]  Song, Chunfeng, Yutaka Kitamura, and Shuhong Li. "Optimization of a novel cryogenic CO2 capture process by response surface methodology (RSM)." *Journal of the Taiwan Institute of Chemical Engineers* 45, no. 4 (2014): 1666-1676.
[14]  AbulHassan "A. Study on desublimation based cryogenic packed beds for CO2 removal from natural gas." PhD, *Universiti Teknologi Petronas*, (2015).
[15]  Donnelly, Harold G., and Donald L. Katz. "Phase equilibria in the carbon dioxide–methane system." *Industrial & Engineering Chemistry* 46, no. 3 (1954): 511-517.